Quantum Electronics **48** (12) 1089–1094 (2018)

https://doi.org/10.1070/QEL16846

Narrowband Raman fibre laser based on a dual-core optical fibre with FBGs inscribed by femtosecond radiation

M.I. Skvortsov, S.R. Abdullina, A.A. Wolf, I.A. Lobach, A.V. Dostovalov, S.A. Babin

Abstract. **The characteristics of Raman lasers based on a dual-core optical fibre are presented. Fibre Bragg gratings (FBGs), selectively inscribed in chosen cores by femtosecond radiation, are used as cavity mirrors. The laser configuration is optimised with respect to the output FBG reflectivity. The possibility of additional spectral filtering, based on the formation of a Michelson interferometer in the laser cavity by inscribing a pair of FBGs in different cores, is demonstrated.**

Keywords: *fibre laser, Raman laser, fibre Bragg grating, femtosecond laser-induced refractive index modification.*

1. Introduction

Lasers based on multicore fibres (MCFs) are promising high-power narrowband radiation sources. When radiation propagates through several MCF cores, the intensity at a specified power decreases, thus reducing the influence of nonlinear effects, which cause lasing spectrum broadening. In designing MCF-based lasers, an important problem is phase locking of the modes propagating in different cores, which is especially urgent when the cores are spaced at large distances. The point is that the modes of different cores are almost independent in this case (because of a weak overlap of their fields). This problem is generally solved using external elements, for example, a Talbot cavity [1] or fibre Bragg gratings (FBGs) inscribed in a multimode fibre with a large core diameter [2].

Lasers based on active multicore fibres have been actively investigated [1–4]. At the same time, to the best of our knowledge, there is only one publication [5] devoted to the laser based on a passive dual-core fibre (DCF), whose gain is due to stimulated Raman scattering (SRS). In that study, a Raman laser with random distributed feedback (RDFB), based on a 550-m polarisation-maintaining (PM) Panda-type DCF, was demonstrated for the first time. The role of a highly reflective mirror in the configuration of a half-open cavity was played by a broadband fibre loop mirror, spliced to the core into which pump radiation was launched. The spectral linewidth of this laser turned out to be five times smaller than the linewidth of a RDFB Raman laser of the same configuration, based on a single-core PM optical fibre: 500 pm at a power of 7 W. It was shown in [5] that the lasing line narrowing in DCFs is due to the weakening of nonlinear effects; this weakening is caused by the increase in the mode effective area and DCF spectral-selective properties, which manifest themselves because of the core mode coupling (the characteristic beating length is 5–10 cm). In the classical scheme of a Raman laser with a loop mirror at the input and a normally cleaved end at the output, which was also implemented by Budarnykh et al. [5], the lasing linewidth in the near-threshold regime was about 1 nm; it increased to 3 nm at an output power of 5.9 W. Other schemes of Raman lasers based on dual- and multicore optical fibres have not been described in the literature; at the same time, the implementation of both random and classical Raman lasers based on this fibre type and study of their characteristics are of great interest.

In this paper, we report the characteristics of different configurations of a Raman laser with a linear cavity formed at the opposite ends of a 550-m-long DCF. The cavity was formed by means of point-by-point femtosecond technique [6], which makes it possible to inscribe selectively FBGs in one or two cores with high positioning accuracy, which cannot be done when gratings are inscribed using UV radiation.

2. Experimental

A dual-core optical fibre was fabricated at the Fiber Optics Research Center of the Russian Academy of Sciences; its parameters are as follows: the fibre core radius is 3 ± 0.3 μm, the average core-to-core distance is 17.1 ± 0.3 μm, the losses at a wavelength of 1.06 μm are 2.2 dB km^{-1}, and the Raman gain at the Stokes wavelength (1.1 μm) is 0.85–0.95 W^{-1} km^{-1} [5].

The general scheme of the configurations under study is presented in Fig. 1. Linearly polarised pump radiation with a wavelength of 1050 nm and power up to 14 W was coupled into one of the DCF cores through a wavelength division multiplexer (WDM).

Splicing was performed using a Fujikura LZM-100 system, which makes it possible to adjust the polarisation axes of spliced PM fibres and perform a desired transverse displacement. A narrowband highly reflective FBG (HR FBG1) was inscribed in the other core near the pump input point. The scheme with core separation for forming a highly reflective mirror in the cavity and introducing pump radiation makes it possible to exclude nonresonant losses of pump radiation at

M.I. Skvortsov, A.A. Wolf, I.A. Lobach, A.V. Dostovalov, S.A. Babin Institute of Automation and Electrometry, Siberian Branch, Russian Academy of Sciences, prosp. Akad. Koptyuga 1, 630090 Novosibirsk, Russia; Novosibirsk State University, ul. Pirogova 2, Novosibirsk, 630090 Russia;
S.R. Abdullina Institute of Automation and Electrometry, Siberian Branch, Russian Academy of Sciences, prosp. Akad. Koptyuga 1, 630090 Novosibirsk, Russia; e-mail: abdullina.sofia@gmail.com

Received 9 October 2018
Kvantovaya Elektronika **48** (12) 1089–1094 (2018)
Translated by Yu.P. Sin'kov

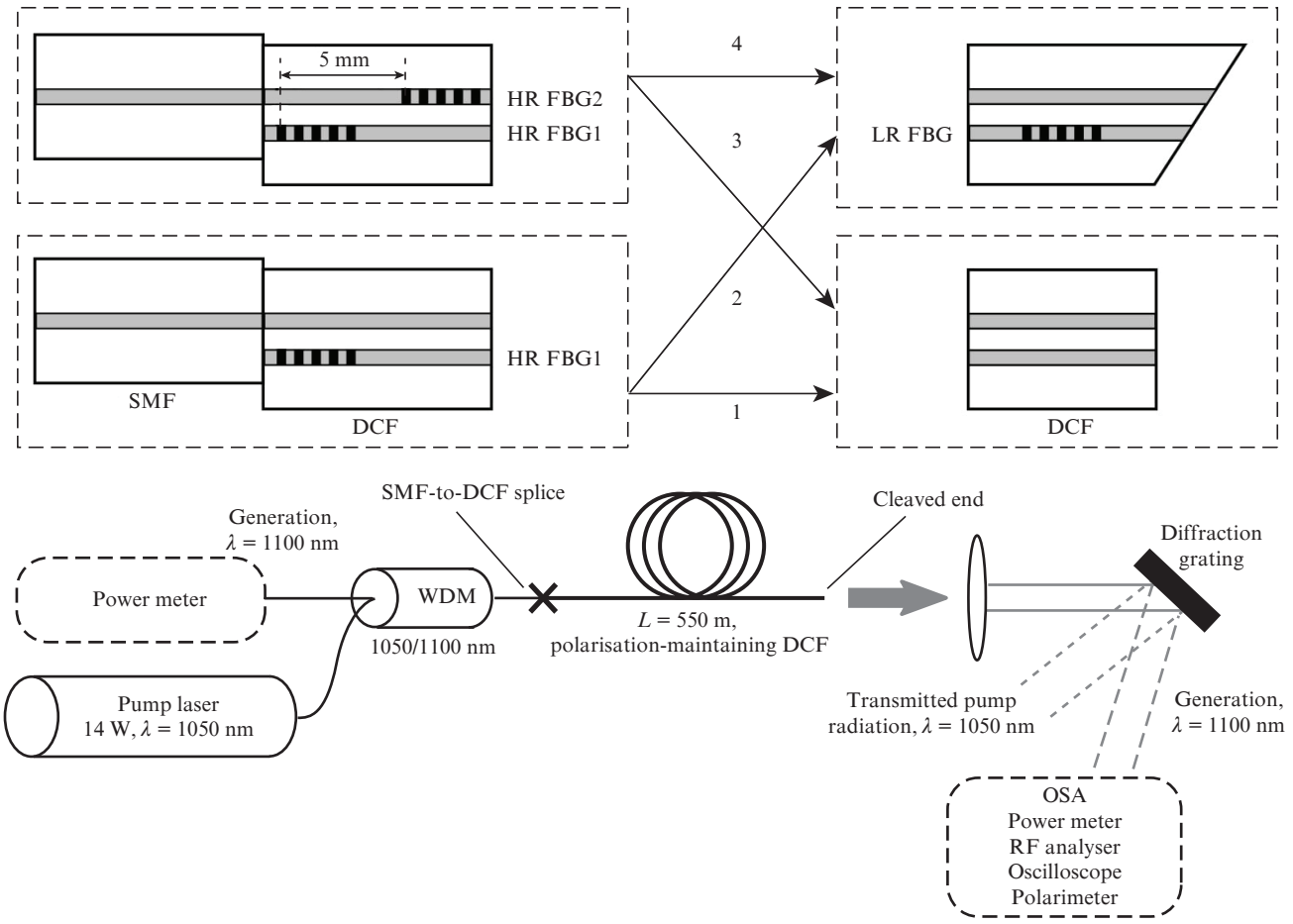

Figure 1. General scheme of the experiment for different configurations (1–4).

the FBG input. Concerning the other DCF end (laser output), either it had a normally cleaved end, or a low reflective FBG (LR FBG) was inscribed on it. Due to the strong core coupling, it was of little importance which of the cores was used to inscribe the output FBG. The input and output FBGs were point-by-point inscribed by femtosecond laser radiation. To provide a high accuracy of FBG positioning inside the MCF, the positions of the cores and modification region were visualised over two coordinate axes oriented perpendicular to the fibre axis [6].

The power of the Stokes component propagating in the direction opposite to the pump radiation direction (i.e., backward) was low in the presented configurations in view of the high reflectivity of FBG1 and large radiation losses at the splices and in the wavelength division multiplexer. Therefore, we considered the characteristics of the Stokes component propagating in the same direction as the pump radiation (i.e., forward). The output radiation was collimated by a lens (Thorlabs F230FC-B) and dispersed by a diffraction grating (Thorlabs GR25-1210). Thus, four spatially separated beams were observed at the output. The lasing spectrum was registered by a Yokogawa AQ6370 optical spectrum analyser (OSA) with a resolution of 20 pm. The radiation modes were studied using an Agilent N9010A RF spectrum analyser; a fast photodetector (a bandwidth up to 1 GHz) and a Tektronix TDS 3032B oscilloscope were applied when measuring dynamic characteristics (power fluctuations). The degree of polarisation was determined with a Thorlabs PAN5710IR2 polarimeter.

Figure 2 shows the characteristics of a Raman laser with a highly reflective ($R_1 \approx 95\%$) narrowband ($\delta\lambda_1 \approx 400$ pm) FBG1 at the cavity input and a normally cleaved end at the cavity output (Fig. 1, configuration 1). The threshold pump power was about 4.7 W, and the maximum generation power for the Stokes component (hereinafter, the total power for both cores) reached 7 W at a pump power of 11.7 W (Fig. 2a). Note that the difference in the maximum pump powers for the configurations analysed here is due to different losses at the splice between the DCF and the single-core single-mode fibre (SMF), which determine the pump radiation power coupled into the cavity.

The solid curves in Fig. 2a correspond to the results of numerical simulation obtained by solving the system of power balance equations for the pump and Stokes power [7] with the boundary conditions taken as point-like reflection at the fibre input (R_l) and output (R_r). Because of the strong coupling between the cores, an FBG with a reflectivity R inscribed in one of the DCF cores is equivalent to a mirror with an effective reflectivity $R_{eff} = R/2$. Thus, for a highly reflective FBG1, one can assume that $R_l = 0.5$. A normally cleaved end in a cavity is equivalent to a broadband mirror with a reflectivity $R_r = 0.04$. The results of numerical simulation with the boundary conditions $R_l = 0.5$ and $R_r = 0.04$ at the gain $g_R = 0.95$ W^{-1} km^{-1} are in good agreement with experimental data (see Fig. 2a). The lasing linewidth (at a level of 3 dB) in the near-threshold regime is about 50 pm; it increases with increasing laser power and reaches 550 pm at the maximum lasing power (7 W) (Fig. 2b). In comparison

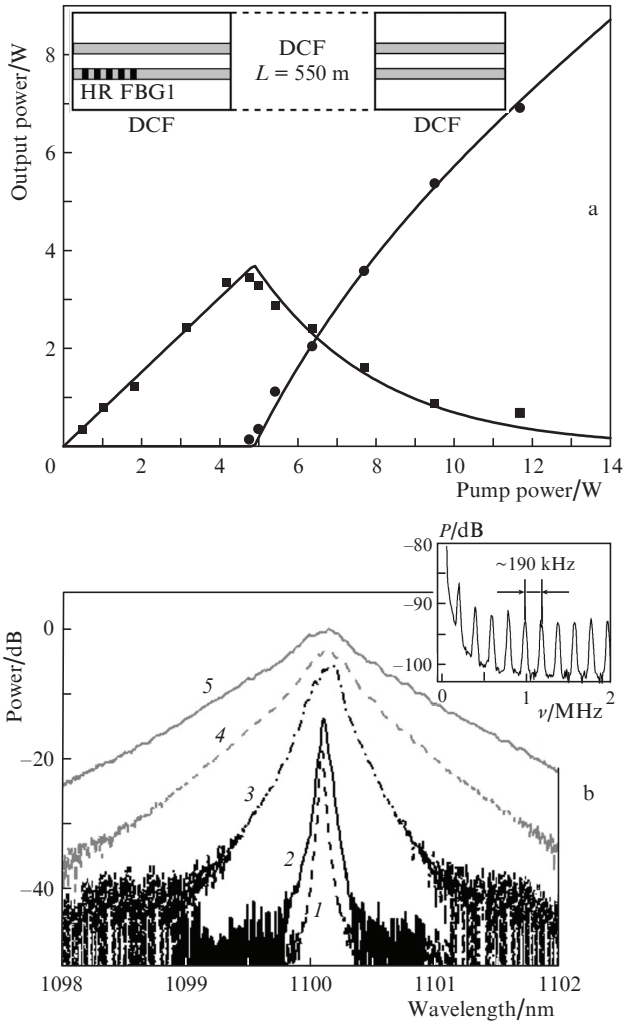

Figure 2. (a) Dependences of the output power of the (■) pump radiation transmitted through DCF and (●) lasing on the input pump power for the cavity configuration with an HR FBG1 at the input and a normally cleaved end at the output (solid lines are the results of numerical simulation) and (b) lasing spectra at output powers of (*1*) 0.1, (*2*) 0.3, (*3*) 2, (*4*) 3.6, and (*5*) 6.9 W. The inset shows the RF spectrum.

with a similar scheme having a loop mirror at the input, the lasing spectrum is significantly narrowed because an FBG with a spectral width of ~400 pm is used instead of a broadband loop mirror in this scheme. The inset in Fig. 2b presents an RF spectrum of output radiation for the cavity configuration with a normally cleaved end. The intermode beating frequency is 190 kHz, which corresponds to a cavity length of 550 m.

To optimise the Raman laser characteristics, the normally cleaved end in the cavity was replaced by a narrowband low reflective FBG. The optimisation was aimed at reducing the threshold pump power without any significant decrease in the Stokes output power. To this end, we calculated the threshold pump power and the output powers of the forward and backward generated beams at a pump power of 12 W and $R_l = 0.5$ for different values of output mirror reflectivity R_r (Fig. 3). The power of the backward Stokes is calculated at the splice between the DCF and single-core fibre. A numerical simulation showed that the strongest decrease in the threshold pump power occurs in the range of values $R_r = 0.05–0.15$; the output lasing power decreases almost linearly in the entire range

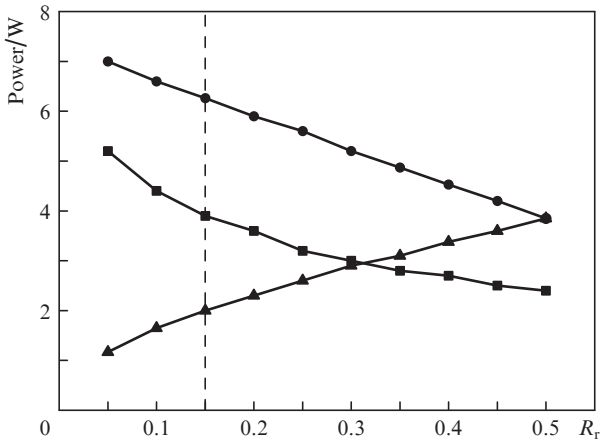

Figure 3. Dependences of the (■) threshold pump power and output powers of the (●) forward and (▲) backward beams on the reflectivity R_r of the cavity output mirror.

of R_r values. Therefore, R_r was chosen to be 0.15 for the experimental laser realisation.

Figure 4 shows the characteristics of a Raman laser, at the output of which an FBG with a reflection spectral width $\delta\lambda \approx$ 120 pm and reflectivity $2R_r \approx 0.3$ is inscribed in one of the cores (Fig. 1, configuration 2). The threshold pump power for this configuration was about 3.5 W, and the maximum lasing power achieved 6.2 W at a pump power of about 11.5 W (Fig. 4a); this value is comparable with the lasing power in the configuration with a normally cleaved end. The results of numerical simulation with the boundary conditions $R_l = 0.5$ and $R_r = 0.15$ obtained at $g_R = 0.85$ W^{-1} km^{-1} are in agreement with the experimental data. The measured linewidth does not exceed 140 pm in the entire radiation power range (Fig. 4b); thus, it is much lower than that in the configuration with a normally cleaved end. The spectra of the cavity-forming gratings HR FBG1 and LR FBG are shown in Fig. 5 by black solid and dashed lines, respectively. The spectral selection in this scheme is due to a narrowband output LR FBG ($\delta\lambda \approx$ 120 pm). Stable lasing was obtained in this configuration due to the FBGs forming the Raman laser cavity, whereas in the scheme of a DCF-based random Raman laser with broadband loop mirror [5] side lobes (spaced at ~0.5 nm) arise and disappear in the lasing spectrum on a time scale of ~1 min; these resonances are related to the spectral selection instability caused by the mode coupling between the cores.

To study the possibility of additional spectral filtering, it was proposed to inscribe two highly reflective FBGs in different cores at the laser input, with a longitudinal displacement along the fibre (HR FBG1,2 in Fig. 1). This configuration leads to the formation of a Michelson interferometer due to the power transfer between DCF cores, as a result of which the spectrum becomes modulated. The distance between the input FBGs along the fibre in this configuration was equal to 5 mm, the FBG length amounted to 3 mm, and the positioning error was less than 1 μm. The reflection spectra of the input HR FBG1,2 are shown in Fig. 5; the spectral widths were measured to be about 400 and 650 pm, respectively. When measuring the FBG1 reflection spectrum, radiation was coupled through a single-core optical fibre spliced to the DCF core, in which a grating was inscribed; when measuring the reflection spectrum of FBG2, a single-core fibre was set closely to the DCF without splicing.

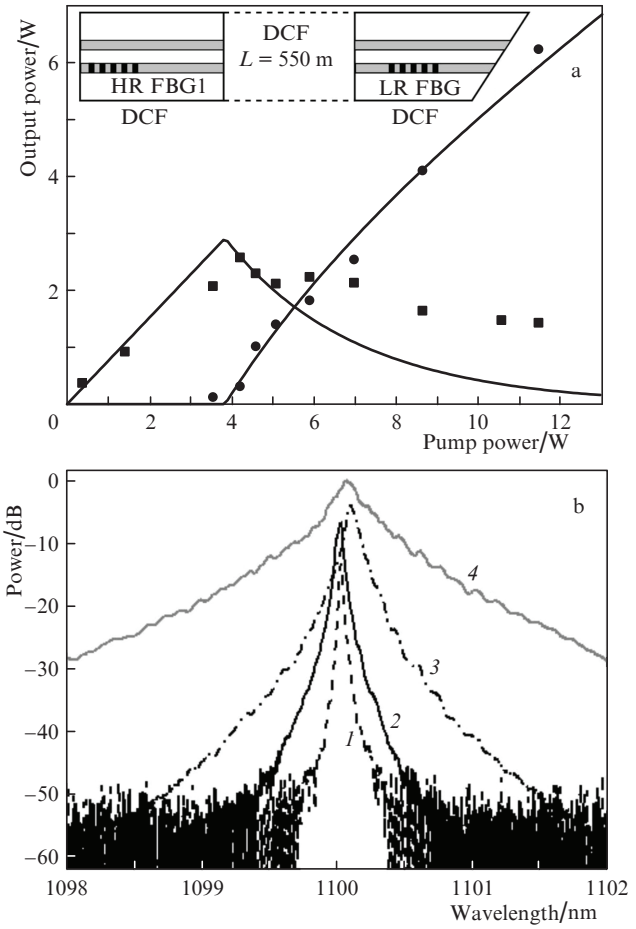

Figure 4. (a) Dependences of the output power of the (■) pump radiation transmitted through DCF and (●) lasing on the input pump power for the cavity configuration with an HR FBG1 at the input and a LR FBG at the output (solid lines are the results of numerical simulation) and (b) lasing spectra at output powers of (*1*) 0.3, (*2*) 1.4, (*3*) 2.55, and (*4*) 6.2 W.

Lasing spectra of a Raman laser with two HR FBGs at the input and a normally cleaved end at the output are shown in Fig. 6b (configuration 3 in Fig. 1) for different output powers. The modulation period in the lasing spectrum near the threshold was 80 pm (Fig. 6b, inset), a value corresponding to the transmission peaks of a Michelson interferometer with an arm length difference of 5 mm. The presence of this structure in the lasing spectrum provides an opportunity for multiwavelength lasing and/or spectral selection of peaks whose width in the near-threshold regime is comparable with the analyser resolution (20 pm). Note that the total lasing spectral width is determined by the reflection spectral width of input FBG1,2 and amounts to about 500 pm (Fig. 6b). The lasing spectrum is unstable in time; energy is redistributed between peaks on a time interval of several seconds. The threshold pump power for this scheme is about 4.5 W, and the maximum power of the Stokes component is 5.4 W at a pump power of 11 W (Fig. 6a). The results of numerical simulation with the boundary conditions $R_l = 0.9$ and $R_r = 0.04$ obtained at $g_R = 0.85$ W^{-1} km^{-1} are in agreement with the experimental data.

To implement additional selection in the laser configuration with two input HR FBGs, a narrowband ($\delta\lambda \approx 120$ pm) low reflective ($2R_r \approx 0.3$) FBG was applied at the laser output (configuration 4 in Fig. 1); its reflection spectrum is shown in Fig. 5 by a dashed curve. The lasing line was significantly narrowed in this configuration (Fig. 7b); the linewidth at output

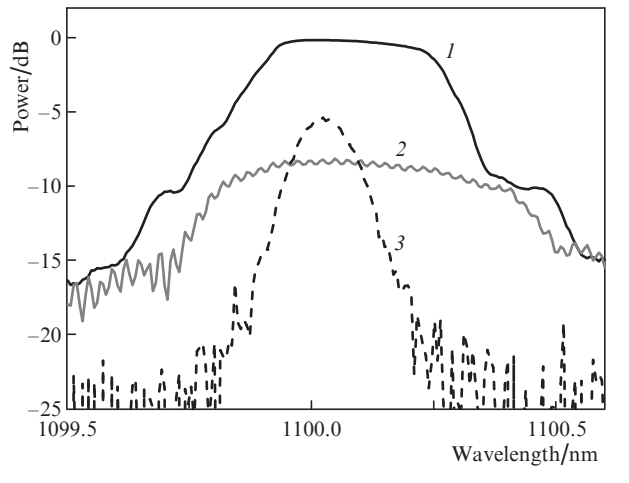

Figure 5. Reflection spectra of the gratings forming the Raman laser cavity: (*1*) HR FBG1, (*2*) HR FBG2, and (*3*) LR FBG.

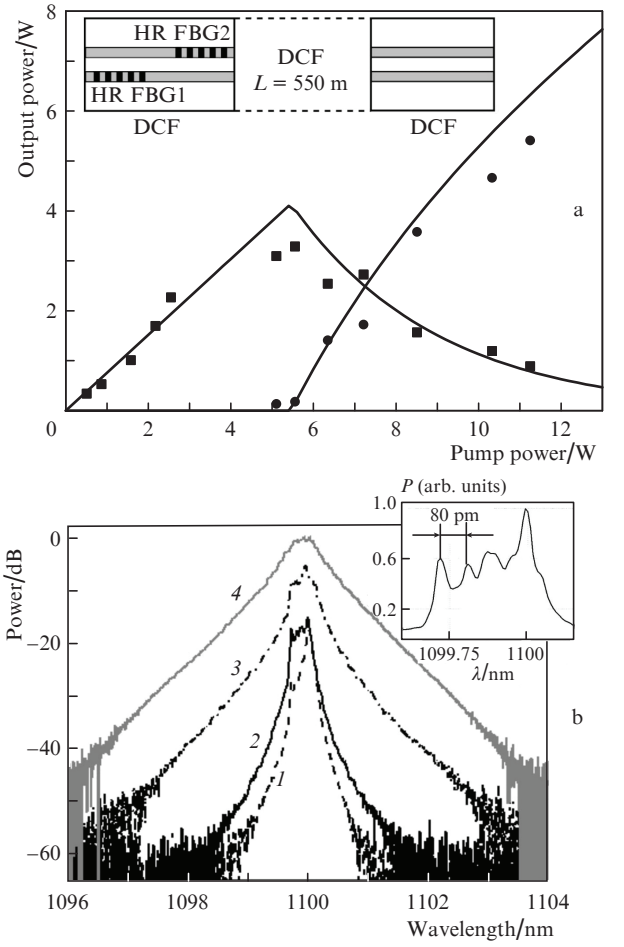

Figure 6. Dependences of the output power of the (■) pump radiation transmitted through DCF and (●) lasing on the input pump power for the cavity configuration with HR FBG1,2 at the input and a normally cleaved end at the output (solid lines are the results of numerical simulation) and (b) lasing spectra at output powers of (*1*) 0.1, (*2*) 0.17, (*3*) 1.7, and (*4*) 5.2 W. The inset shows the lasing spectrum at an output power of 0.17 W (linear scale).

powers below 2 W did not exceed 100 pm. The pump power threshold was about 2.5 W, and the maximum Stokes component power was 5.5 W at a pump power of 8.5 W (Fig. 7a). The results of numerical simulation with the boundary conditions $R_l = 0.9$ and $R_r = 0.15$ obtained at $g_R = 0.85$ W^{-1} km^{-1} are in good agreement with the experimental data.

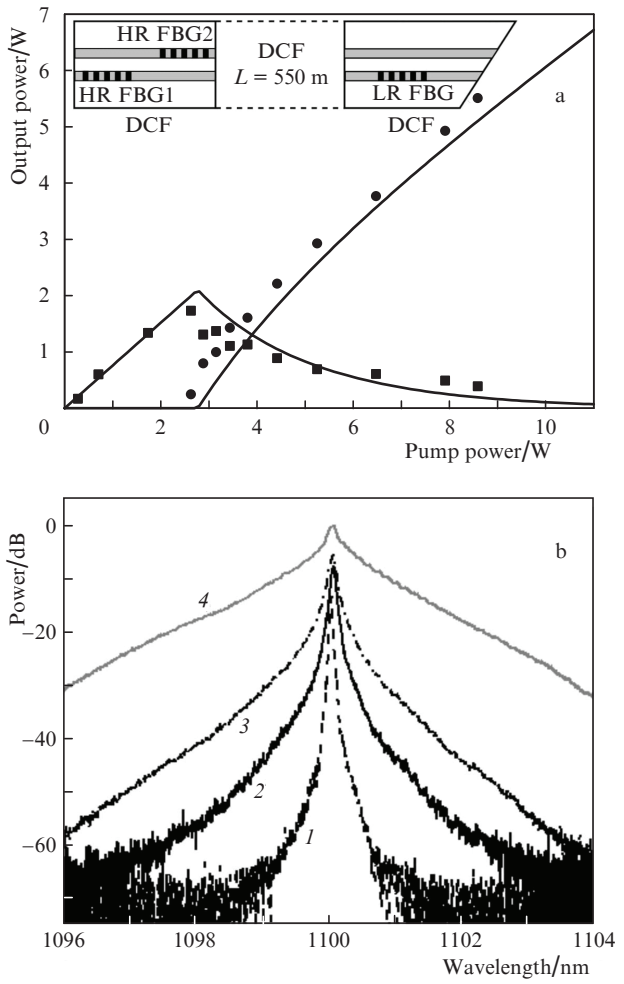

Figure 7. Dependences of the output power of the (■) pump radiation transmitted through DCF and (●) lasing on the input pump power for the cavity configuration with HR FBG1,2 at the input and a LR FBG at the output (solid lines are the results of numerical simulation) and (b) lasing spectra at output powers of (*1*) 0.25, (*2*) 1, (*3*) 1.6, and (*4*) 5.5 W.

The lasing linewidths for different laser configurations are compared in Fig. 8. In the configuration with one HR FBG at the input and a normally cleaved end at the output, the lasing line uniformly broadens from 50 pm at a lasing power of 100 mW to 500 pm at an output power of 7 W. Using a LR FBG instead of a normally cleaved end, we could obtain minimum lasing line broadening (140 pm) at the maximum output power (6.2 W). The configuration with two input HR FBGs and a normally cleaved end at the output provides the strongest lasing line broadening: the total linewidth rapidly grows at low powers and exceeds 500 pm at an output power of 1.5 W. The configuration with two HR FBGs at the input and a LR FBG at the output yielded the narrowest line at low output powers (less than 50 pm at an output power of ~1 W).

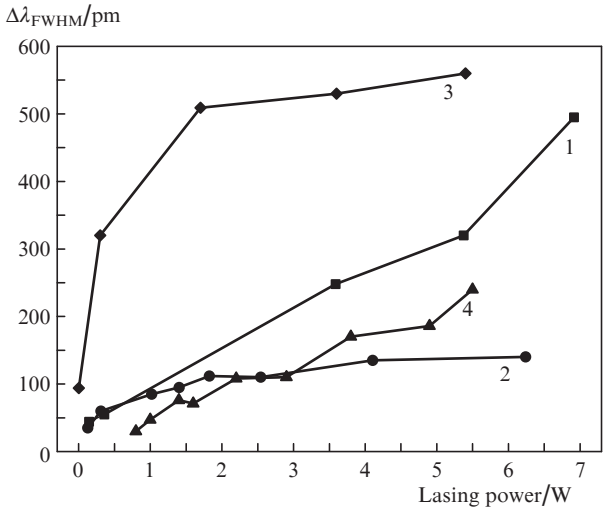

Figure 8. Dependences of the Raman laser linewidth on the Stokes component power for different laser configurations: (1) HR FBG1 at the input and a normally cleaved end at the output, (2) HR FBG1 at the input and a LR FBG at the output, (3) HR FBG1,2 at the input and a normally cleaved end at the output, and (4) HR FBG1,2 at the input and a LR FBG at the output.

The maximum output lasing power was obtained in the configuration with one HR FBG and a normally cleaved end at the output (7 W at a pump power of 11.7 W). The most efficient pump-to-Stokes conversion (about 65%) was obtained in the scheme with two HR FBGs at the input and a LR FBG at the output (5.5 W at the output at a pump power of 8.5 W).

The thus obtained Stokes radiation is continuous-wave. Since pump radiation was linearly polarised, and polarisation-maintaining fibre and components were used in the experiment, the Stokes radiation was also linearly polarised. The extinction ratio, measured with a Thorlabs TPX 5004 polarimeter in the configuration with two input HR FBGs and a normally cleaved end at the output, turned out to be about –20 dB.

3. Conclusions

The characteristics of DCF-based Raman lasers, where FBGs inscribed by femtosecond radiation played the role of cavity mirrors, were investigated. The scheme with one HR FBG at the input was optimised with respect to the output LR FBG reflectivity, as a result of which the lasing line was significantly narrowed as compared to the configuration with an HR FBG at the input and a normally cleaved end at the output (at similar values of maximum output power). In this configuration, the linewidth depends weakly on power and does not exceed 140 nm, which is smaller by a factor of about 4 than the lasing linewidth of an RDFB laser in the configuration with a loop mirror (550 pm), at a comparable output power (~7 W), and is an order of magnitude smaller than the linewidth obtained in the classical configuration with a loop mirror at the input and a normally cleaved end at the output (3 nm at 5.9 W), implemented by Budarnykh et al. [5]. The parameters of this narrowband lasing correspond approximately to the best results obtained for a short Raman laser based on a PM single-mode fibre with special narrowband FBGs [8].

The highest optical efficiency (65%) of pump-to-Stokes conversion was achieved for the scheme with two HR FBGs at the input and a LR FBG at the output; it slightly exceeded the efficiency of conventional Raman fibre lasers with narrowband FBGs [8].

The application of multicore fibres when developing Raman fibre lasers makes it possible to reduce the influence of nonlinear effects and, correspondingly, greatly decrease the lasing spectral broadening at the same output power. The application of point-by-point FBG inscription technique makes it possible to avoid nonresonant losses for the pump radiation launched into cavity and form structures providing an opportunity for additional selection.

Acknowledgements. We are grateful to the Multiple-Access Centre "High-Resolution Spectroscopy of Gases and Condensed Matter" at the IA&E SB RAS, Novosibirsk, for the supplied equipment and to A.A. Vlasov for the help in experiments.

This work was supported by the Russian Science Foundation (Grant No. 14-22-00118).

References

1. Wrage M., Glas P., Fischer D., Leitner M., Vysotsky D.V., Napartovich A.P. *Opt. Lett*., **25**, 1436 (2000).
2. Kurkov A.S., Paramonov V.M., Dianov E.M., Isaev V.A., Ivanov G.A. *Laser Phys. Lett.*, **3**, 441 (2006).
3. Kurkov A.S., Babin S.A., Lobach I.A., Kablukov S.I. *Opt. Lett.*, **33**, 61 (2008).
4. Boullet J., Sabourdy D., Desfarges-Berthelemort A., Kermène V., Pagnoux D., Roy P., Dussardier B., Blanc W. *Opt. Lett*., **30**, 1962 (2005).
5. Budarnykh A.E., Lobach I.A., Zlobina E.A., Velmiskin V.V., Kablukov S.I., Semjonov S.L., Babin S.A. *Opt. Lett.*, **43**, 567 (2018).
6. Dostovalov A.V., Wolf A.A., Parygin A.V., Zyubin V.E., Babin S.A. *Opt. Express*, **24**, 16232 (2016).
7. Vatnik I.D., Churkin D.V., Babin S.A. *Opt. Express*, **20**, 28033 (2012).
8. Surin A.A., Borisenko T.E., Larin S.V. *Opt. Lett.*, **41**, 2644 (2016).